4. Geometry and evolution of the Düzce fault zone

In this chapter are first illustrated which stratigraphical, tectonical and geomorphological features were surveyed and mapped, then are described, progressively zooming out: 1) exemplary aspects of the Düzce fault zone along a key area; 2) the overall Düzce Fault coseismic and short- (Holocene) and long-term (Pliocene-Pleistocene) geomorphic expression; 3) the relationships of the Düzce fault segment with the nearby Karadere fault section.

4.1. Mapping the Düzce Fault

The first step undertaken for the investigation of the Düzce fault activity is geological and geomorphological mapping of about 160 km^2 at 1:20,000-scale. The mapping was carried out by integrating and detailing the published 1:100,000 scale geological maps [Herece and Akay, 2003]. This map was completed differentiating with particular attention the units of the recent continental deposits cover and tracing in detail the 1999 coseismic ruptures. As topographic base we used a 2.5m-resolution, orthorectified SpotView Image, draped with 1:25,000 scale, 10-m-equidistance, digital contour lines. A 20-m-resolution Digital Elevation Model (DEM, interpolated from 1:25,000-scale topography), and standard morphometric derivatives (hill-shaded and slope angle maps) were produced by means of a spatial analysis and display software (Vertical Mapper3.0). Geomorphological observations all supported by field survey comprise (1) paraglide-aerial (ultra-light aircraft, fig. 4.1.1) photographs, which permitted observations at larger scale then the conventional aerial photo and also to obtain oblique view of the territory, (2) 1:18,000 and 1:35,000 scale aerial photographs, (3) DEM and (4) satellite remote sensing data processed using the ER-Mapper and ERDAS software. The field survey data were collected and geo-referenced by means of handle Global Positioning System (GPS) and, together with the remote-sensing data, were organized and displayed on maps using a Geographic Information Systems (GIS, MapInfo7.0).

Figure 4.1.1. Motorized equipment (left) utilized for paraglide (right)-aerial photography.

In the following the main stratigraphic, tectonic and geomorphological features presented on the map (Plate 1) are illustrated.

4.1.1. Stratigraphy

The pre-Neogene basement (Ordovician-Middle Eocene) of the region consists of sedimentary and low-grade metamorphic rock assemblages of the Istanbul Unit, unconformably overlain by marine basins and volcanic rocks (Mastrichtian-Middle Eocene) [Şengör and Yılmaz, 1981; Okay, 1989; Yılmaz et al., 1995]. Along the Almacik block, south of the study area, the Istanbul Unit participates in the Oligocene Intra-Pontide suture, together with the Sakarya Unit, that is made up of a metamorphic basement and of Jurassic-Cretaceous sedimentary cover [Okay, 1989; Yılmaz et al., 1995].

In the study area the stratigraphic sequence of the bedrock has been mapped following the subdivision of Herece and Akai [2003], and the outcropping formation are:

1) Basins developed on the Istanbul (Pontide)-Sakarya mélange

- Andesitic-basaltic rock units (Middle-Late Eocene)
- Sandstone-shale and conglomerate unit (Middle-Late Eocene)
- Sandstone-shale unit (Early-Middle Eocene)

- Sandstone-conglomerate unit (Maastrichtian-Paleocene)

2) Istanbul Unit:

- Granitoid unit (Paleozoic-Jurassic)
- Arkosic conglomerate, purple siltstone and fossiliferous siltstone units (Early Devonian)
- Limestone-Sandstone unit (Silurian-Devonian)
- Sandstone-conglomerate unit (Ordovician-Silurian)

In northwest Turkey, all of the basement units are unconformably covered by Neogene deposits. Between the Izmit gulf and the Düzce basin the deposits range in age from the end of the Middle Miocene to the Holocene, and were deposited in different units separated by unconformities. Studies on the Düzce basin Neogene sequence are scarce in the literature and, as a consequence, detailed information about its character and origin is missing. The best known stratigraphic sequences of the area are referred to the nearby Akyazi basin (fig.3.2.14), west of the Düzce basin, where the oldest infill is dated Late Pliocene (Emre et al., 1998; Unay et al., 2001). According to these Authors, the Late Pliocene-Quaternary sediments of the Akyazi Basin rest on the pre-Neogene rocks with angular unconformity and are divided into three stratigraphic units: 1) Holocene alluvium, alluvial fan and fan delta sediments; 2) Middle Pleistocene-Holocene fillings of alluvium, alluvial fan and fluvial deposits; 3) Late Pliocene-Middle Pleistocene sedimentary unit (Karapürçek formation) of alluvial fan, fluvial, flood plain deposits that unconformably is overlain by the Middle Pleistocene-Holocene deposits (fig. 4.1.2).

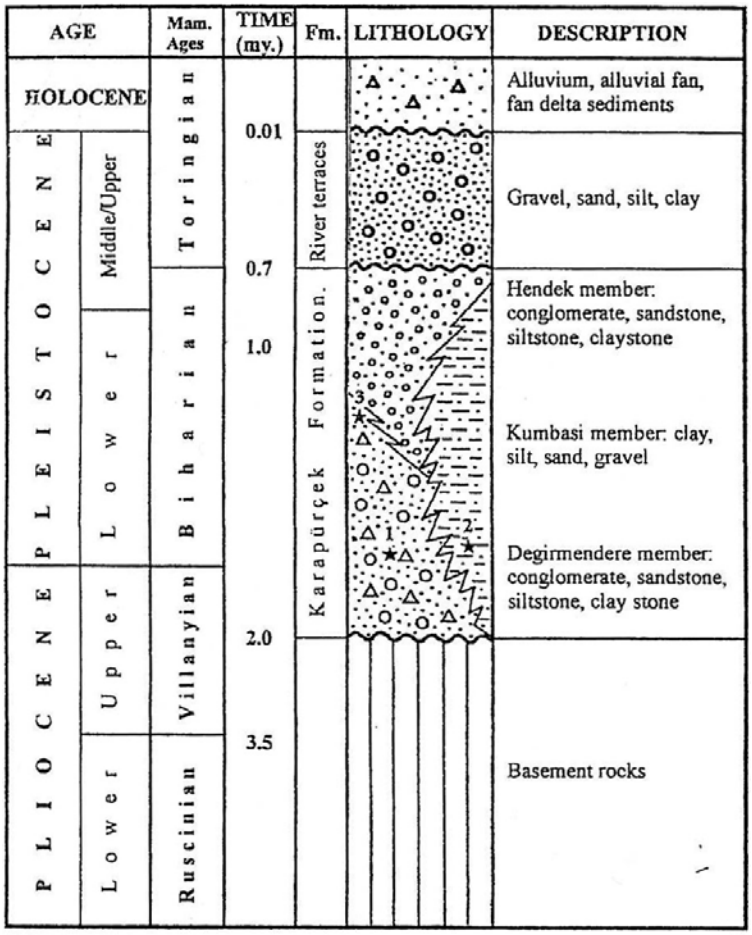

Figure 4.1.2. Columnar stratigraphic section of the Late Pliocene-Quaternary deposits of the Akyazi basin. (from Emre et al., 1998).

During the field geological survey, the following continental deposits were recognized at several outcrops and the sedimentary bodies were mapped on the basis of their morphological features:

- Slope Debris (Holocene-active):

  Unsorted, clast-supported deposits of angular debris, boulders and cobbles, from nearby rock outcrops. Fine, oxidized red and yellow matrix with sand, and gravels, from stratified to unstratified. Forming coalescent fans on lower slopes and valleys. Occuring on higher slopes as talus near bedrock outcrops and escarpments.

- Colluvial and eluvial deposits (Holocene-active):

  Unsorted, unstratified matrix-supported deposits of angular debris. Fine, oxidized red and yellow clay matrix with sand, and rare gravels. Locally assuming a character of slope-wash

and residual deposits, derived by in situ weathering or accumulation with limited transportation.

- Fluvial deposits (Holocene-active):

Unconsolidated, silt and sand with common open-washed, embricated and well-rounded cobbles, and big boulders along streams and alluvial valleys. Sediments well to poorly stratified with gravelly braided channel deposits consisting of many cut and fill features.

- Alluvial deposits (Holocene-active):

Unconsolidated stratified brown, gray colored silty and clayish flood deposits with yellow sand and polycyclic open-washed levels of embricated and rounded pebbles and rare cobbles, deposited by rivers during flooding events (overbank deposits) (fig. 4.1.3).

Figure 4.1.3. Outcrop of the Holocene Alluvial deposits of the Kaynasli basin along the Asarsu river.

- Alluvial fan deposits (Holocene-active):

Fan-shaped deposits of water-transported material (alluvium). Composed by unconsolidated silt, sand, rounded and sub-rounded pebbles (fig. 4.1.4) and cobbles, mostly well stratified, with small boulders along the main channel. Coarse-grained at the fan

mouths relatively fine-grained at the edges. Forming at the base of marked break in slope and related to the present drainage system dynamics.

Figure 4.1.4. The Holocene alluvial fan deposits with alternated silt, sand, and sub-rounded pebbles near Cinarli.

- Alluvial fan deposits (Holocene):

Water-transported material composed by unconsolidated and well stratified red-brown silt and sand, and oxidized rounded or sub-rounded cobbles and boulders (figs. 4.1.5 and 4.1.6). Forming at the base of marked breaks in slope and no more related to the present drainage system dynamics. Deeply entrenched by the main channel and indented by erosional terraces that occasionally dissect the original fan shape. Locally they have thin weathering rinds.

Figure 4.1.5. View of Holocene alluvial fan deposits of a terrace near Yenikoy.

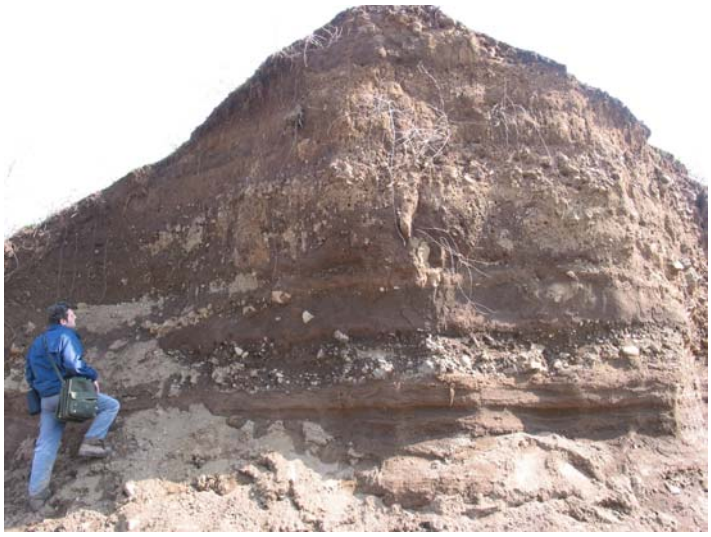

Figure 4.1.6. Outcrop of stratified silt and a pebbles of Holocene alluvial fan deposits near Yenikoy.

- Alluvium and Alluvial fan deposits (Late Pleistocene):

Unconsolidated, poor to well stratified, largely oxidized deposits of red-yellowish sand, silt and red-brown and gray clay, with well rounded pebbles (fig. 4.1.7 and 4.1.8). Located in embayments at the base of the mountain front, where they coalesce forming bajadas. Severely eroded with occasional dissection of the original depositional surface, with entrenchments and superimposition of more recent alluvial deposits. No more related to the present drainage system dynamics and forming low-energy landscapes suspended on the present-day Düzce basin.

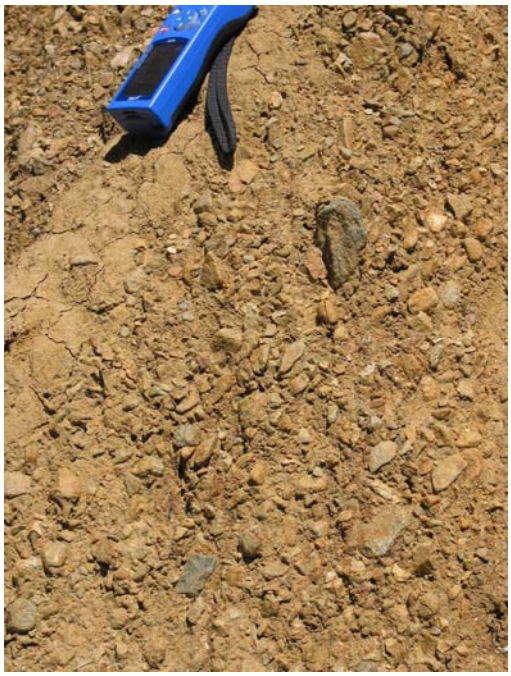

Figure 4.1.7. Well stratified and oxidized silt and sand with rounded pebbles near Beykoy.

Figure 4.1.8. Oxidized sand with rounded pebbles and gray clay near Yenikoy.

- Alluvial fan deposits (Middle Pleistocene?- Late Pleistocene):

Top member of the Karapürçek formation. Sequence of loose deposits with red, brown and yellowish-colored silty matrix and poorly sorted lithology with pebblestone, sandstone, mudstone and siltstone (fig. 4.1.9).

Figure 4.1.9. Poorly stratified and sorted Middle-Late Pleistocene deposits, with low evolution of pebbles.

-Alluvial fan deposits (Early Pliocene- Late Pleistocene?):

Basal member of the Karapürçek formation. Sequence of poorly sorted yellow and brown colored sandstone, siltstone and dark gray, black claystone, with numerous gray, beige-yellowish pebbles and cobbles of Paleozoic to Eocene formations (fig. 4.1.10).

Figure 4.1.10. Outcrop of basal member of Pleistocene Karapürçek formation near Yenikoy.

4.1.2. Tectonic structures

In the 1:20.000 map (Plate 1) different faults sets are reported with different colours.

Red faults represent the faults rupturing during the November 12, 1999 Düzce earthquake, whose surface expression was still evident during the past four years. These faults represent the sites of localized coseismic deformation, that appears as single fractures as well as mole-tracks or mixture of these.

Orange traces are surface fault ruptures occurred during the August 17, 1999 Izmit earthquake, and have been compiled from the available literature (Barka et al., 2002; Lettis et al., 2002; Hartleb et al., 2002; Komut, 2005). Most of the ruptures that occurred on the flood plain are composed by tension fractures.

Black faults indicate tectonic structures that, even though did not ruptured coseismically during the 1999 seismic sequence, present evidences of Quaternary activity. These faults, that affect mostly the bedrock formations, were drawn by means of aerial-photo interpretation and checked at several outcrop spots (Appendix I-III; *e.g.*, fig. 4.1.11).

Figure 4.1.11. Outcrop of the tectonic contact between the sandstone-shale and conglomerate unit (Middle-Late Eocene, lower left) and the sandstone-shale unit (Early-Middle Eocene, on the right).

In the following, the terminologies used in the text and referred to different connotations of the word “fault” are clarified.

Fault strand (or splay, stretch): Generic term indicating individual faults of a set of closely-spaced, parallel or sub-parallel branches of a fault system.

Fault segment: The entire length of major faults do not always rupture at one time to create a single major earthquake. Fault segment indicates a discrete fraction of the total fault length, separated by recognizable boundaries, that tends to independently rupture causing an earthquake.

Fault section, subsection, element: Any partition, partial component or piece of a fault segment along its length. Each term refers to different scales of subdivision, from the smaller (section) to the larger (element). These subdivisions are designated on the basis of the uniformity of their structural or morphological character (strike, kinematics, topographical change, short/long-term tectonic expression, etc.).

4.1.3. Geomorphology

Geomorphological observations are reported on the map to provide additional information that is not highlighted by the low resolution topographical base.

- Drainage:

  Drainage was drawn starting from the analysis of aerial-photos and refined by field survey, including also small streams and ponds in the area along the 1999 surface ruptures. Field survey and data from the map of the Düzce Water Management Institute helped to correctly represent the state and location of artificial channels, which have been affected by coseismic deformations. Coseismic and short/long-term deflections of the streams crossing the 1999 coseismic fault trace (fig. 4.1.12) were measured by using a tape measure and/or portable GPS instruments (when the deformation was within its error of measure), in order to reconstruct the distribution of short/long-term strike-slip offset (Chapter 5 and Appendix I-I.v). Lake Efteni is characterized by a fluctuating shoreline.

According to the season and idrological balance, the lake occupies a perennial small area (dark blue) that can expand on the Düzce plain (light blue).

Figure 4.1.12. Aerial view of a deflected stream.

- Terrace risers, scarps and scarp bases:

Scarps on Quaternary deposits or bedrock, induced by both tectonics and erosion, are reported on the map. Terrace risers, that are downcut on alluvial and fluvial deposits due to response of the stream profile to lowering of local base level, are drawn in blue. Tectonic or generic scarps incised on both Quaternary deposits or bedrock are drawn in brown and have been differentiated with different symbols in three classes, according to their height. To better visualize the slope gradient and breaks and to highlight the location of the scarps higher than 3 m, scarp bases are also reported (fig. 4.1.13). The degree of landform development (scarp evolution) and weathering helped in estimating the relative ages of the Quaternary deposit surfaces (the operative assumptions are summarized by Pierce and Colman (1986) and include homogeneity of parent material, homogeneity of process, and recognition of the importance of initial scarp height, scarp aspect, and time

in the evolution of scarps). In order to reconstruct the distribution of short/long-term dip-slip offset of the 1999 Düzce fault trace (Plate 1b), each of the well-defined tectonic scarps reactivated by the surface faulting was quantified by means of topographic profiles using a tape measure and Abney level.

Figure 4.1.13. View of a ridge flank. Green symbol indicates ridge hingeline, brown symbols indicate scarp edge (triangles) and scarp base (v).

- Ridges, saddles and peaks:

These are smoothed features (mapped with green colors) that are witnesses of paleo-landscapes due to morpho-genetic processes or are related to tectonic. The hingeline of saddles and ridges have been reported and, in order to picture asymmetrical ridges and warps, slopes have been differentiated between gentle (<30°, light symbol) and steep (>30°, heavy symbol). Reliable tectonic ridges are those located in the near-fault, that present a trend of their elongation paralleling the fault trend, coherently with the finite deformation on fault simple shear (see Chapter 2.1.1) (fig. 4.1.13). These grew due to local transpression and diffuse deformation of loose deposits, creating anomalous topography on the hosting deposits. Others tectonic ridges are those that developed as shutter ridges, having an effect on the drainage pattern.

- Landslides:

Landslides have been subdivided in two type. Those that have been triggered or reactivated by the 1999 seismic sequence (red), that showed new tear ruptures and

renewal of crowns. Those that present clear Holocene activity but are still quiescent (black). The study area show widespread distribution of latest gravitational phenomena along the 1999 coseismic surface faulting, with landslides bodies from tens up to hundred of meters wide. Along the western part of the Almacik rangefront, is evident a large presence of Holocene landslides, hundred of meters wide, whereas a 2km-wide Holocene landslide set foot in the eastern part of the Kaynasli basin.

- Paleosurfaces (Pliocene-Holocene):

Depositional or erosional elevated relics and remnants of large planation surfaces at different elevations were mapped too. They are "inherited" from a previous landscape that it was not exclusively shaped by the currently active erosional system. These surfaces display a different architecture and grade of preservation according to their age and elevation, but the correlation between different surfaces was not an object of the this thesis (fig. 4.1.14).

Figure 4.1.14. Aerial view of two paleosurfaces (top left and lower right).

- Tilt:

The probable slight roll of surfaces has been symbolized by arrows, with their tip pointing toward the plunge. Most of the tilts have been recognized on the base of anomalous dip of surfaces with respect to the general depositional and erosional environment, few tilts have been recognized on the base of direct observation of deformed deposits.

- Flatirons:

Flatirons have been mapped on the base of aerialphoto interpretation. The erosional processes acting on the range front, gave place to triangular or trapezoidal relict slopes facets, separated by strong incisions of drainages flowing orthogonally to the range front. The flatirons are generated when there is a significant alteration in the morphogenesis of the slope involving the change towards a prevalence of incision processes (Büdel, 1982) that can derive from both tectonics (active fault , with dip-slip component, at their foot) or lowering of the local drainage basal level. The best preserved flatirons are those NE-facing, observed along the western part of the study area.

4.2. Detailed study of the Düzce Fault Zone

Exemplary features of a key area between Efteni lake and Beykoy village, where the coseismic ruptures affect mainly Quaternary deposits, are described: (1) the patterns of the coseismic ruptures at different scales; (2) the short/long-term fault patterns that are derived from cumulative tectonic landforms, along the coseismic ruptures and at a broader area around them.

4.2.1. Coseismic ruptures

The 1999 earthquake ruptures between Efteni Lake and Beykoy (fig. 4.2.1) were mapped in detail, collecting data on: a) structural patterns of fractures and faults; b) geomorphic modifications induced by the earthquake; c) coseismic offset of piercing points such as roads, fences, tree lines,

channels, streams, buildings, etc. (~80 new measurements, additional to those made by Akyuz et al. [2000 and 2002] soon after the earthquake, see Appendix I-I.i and I-I.ii).

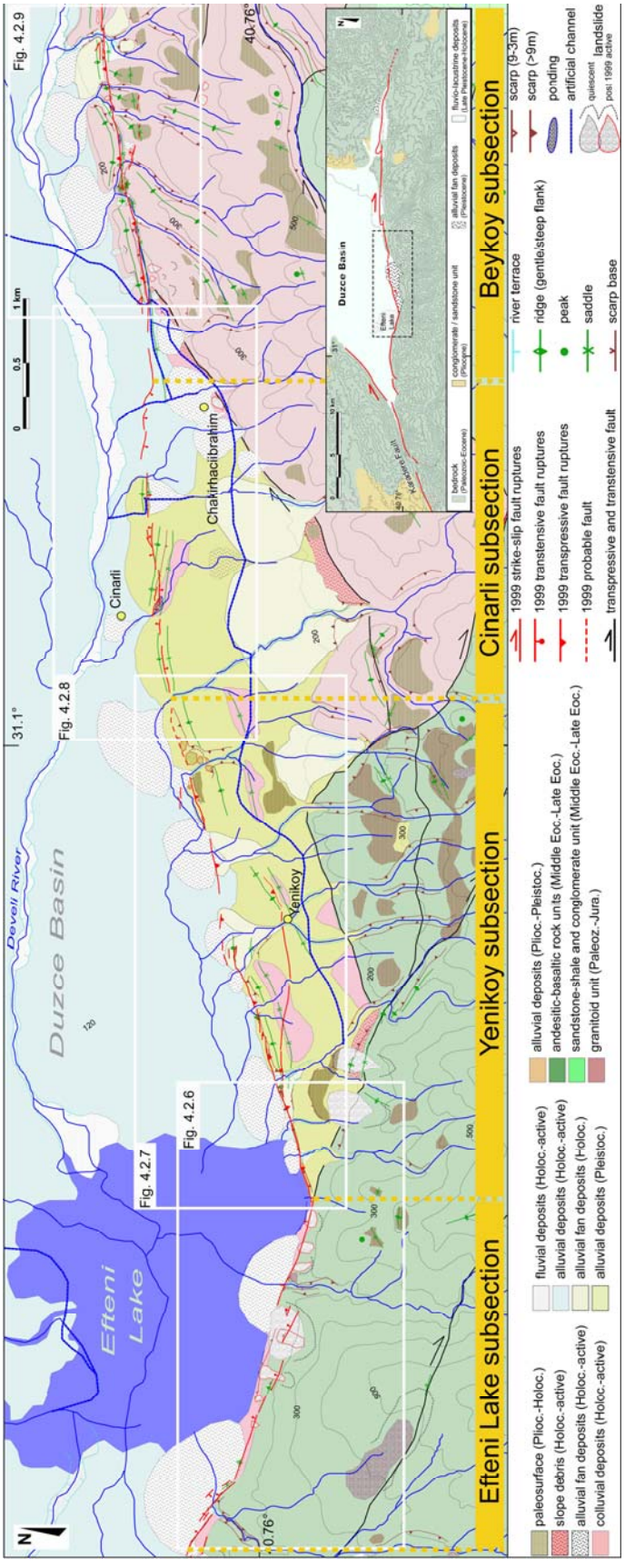

Figure 4.2.1. Geological map of the study area. Continental deposits and coseismic fault trace from 1:25.000 scale field survey, bedrock formations from Herece and Akay (2003). Rectangles define the location of figures 4.2.6 to 4.2.9. Contour interval 100 m. See dashed rectangle in the inset for location.

4.2.1.1. Structural pattern and geomorphic modifications

The expression of the 1999 coseismic ruptures is predominantly mole-track type. Each mole-track deformation zone, 0.5 to 5 m-wide (occasionally becomes complex and its width increases up to 50 m) and 30-100 m long, is referred in the following text and figures as a single displacement zone (SDZ) and is the morphological expression of a complex dextral fault zone, mainly consisting of synthetic, 1-10 m-long, strike-slip Riedel shears (fig. 4.2.2). These features are typical of poorly consolidated sediments (*i.e.*, continental Quaternary deposits) that overlay a rigid bedrock (*i.e.*, Paleozoic-Eocene bedrock), as observed by Riedel [1929] in analogical deformation experiments. The main characteristics of the system are an over-stepping, en-échelon array of left-stepping synthetic Riedel shears (R-shears) and a right-stepping array of compressional fold axes (fig. 4.2.2b and c).

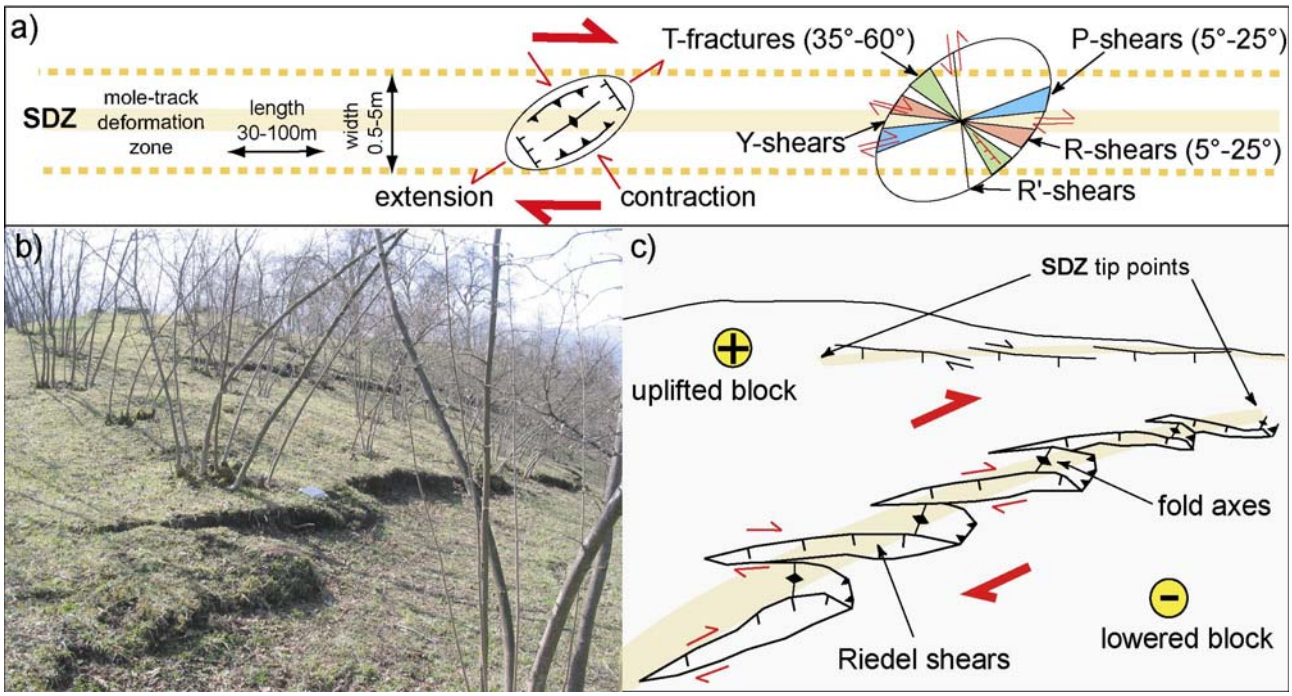

Figure 4.2.2. a) Sketch of typical dextral single displacement zone (SDZ) and its approximate size. Outcrop scale structural elements are drawn along with the relative angle of deviation from the SDZ. b and c) oblique photo and sketch of a single displacement zone (SDZ) in the study area.

Antithetic Riedel shears (R'-shears) are rarely observed even in the transfer zones at the R-shears step-overs where they would be expected, instead. At places, where the width of the deformation zone increases, Riedel systems develop a second array of right-stepping synthetic

shears (P-shears or Thrust-shears, fig. 4.2.3), that locally join or end up to the R-shears [*e.g.*, Tchalenko, 1970; Wilcox et al., 1973; Naylor et al., 1986]. At a few sites, the zone of deformation consists not only of a set of en-échelon R-shears, but also P-shears together with compressional fold axes. Here, P-shears have grown and linked to R-shears, forming shear lenses, and afterwards Y-shears have also developed, in a typical anastomosing pattern of a through-going wrench fault, parallel to the SDZ [*e.g.*, Woodcock and Schubert, 1994; Naylor et al., 1986] (fig. 4.2.3). Locally, arrays of fractures form as well, with a prevalent extensional kinematics (T-fractures).

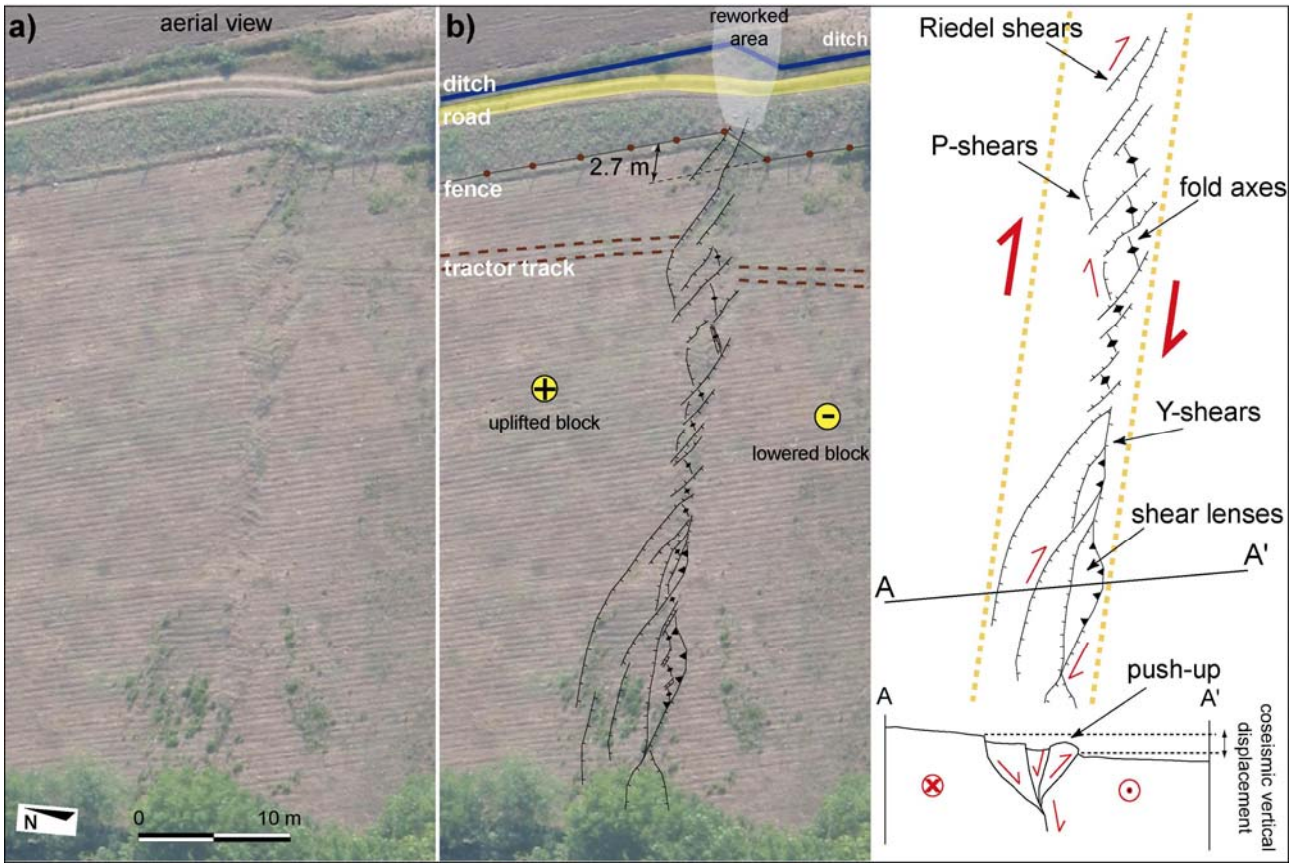

Figure 4.2.3. a and b) Aerial view of typical anastomosing pattern of a single displacement zone (SDZ) and simplified sketch map (c), coupled with not-in-scale topographic profile (see fig. 4.2.6 for location).

At smaller scale, the 30 to 100 m-long SDZs themselves are also organized in slightly overlapping en-échelon arrays. At this scale the SDZs constitute a left-stepping synthetic Riedel system spaced 3 to 20 m, which shows a clear continuity for a length of 300 to 800 m. The envelope of this en-échelon array defines a principal displacement zone (PDZ) that has a strike

direction diverging 5°-10° from the SDZ and produces a topographic offset with the consistent uplift of one of the fault blocks (fig. 4.2.4). The alignment of the PDZs defines the average location, strike and relative movement of the 1999 coseismic surface fault trace (CFT) of each subsection of figure 4.2.6a in which it is located.

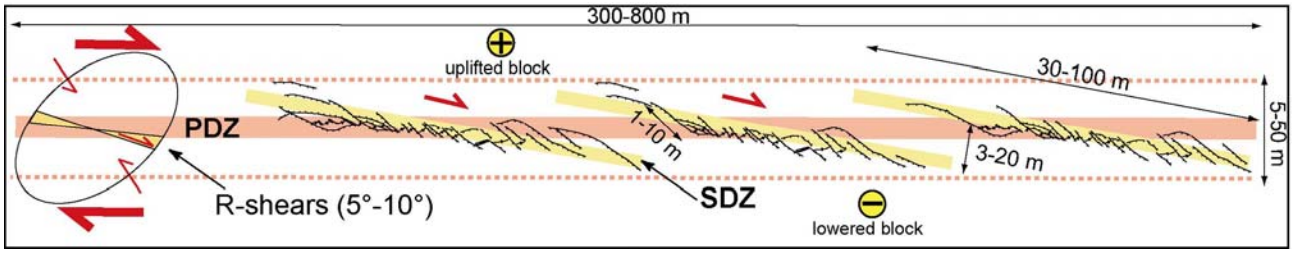

Figure 4.2.4. Sketch of the en-échelon arrays formed by single displacement zones (SDZ), whose envelope represents a principal displacement zone (PDZ). Note the approximate size in relation to figure 4.2.3.

4.2.1.2. Coseismic offsets

The offset measurements were collected paying attention in separating single from multiple slip events. The 1999 offsets were mostly measured using recent manufact that were cross-cut by the still visible mole-tracks. These manufact provide reliable piercing points for both horizontal and vertical offsets (fig. 4.2.5). Vertical displacements on the 1999 free face at locations were measured where the possibility of apparent vertical displacements due to juxtaposition of topographic features (*i.e.*, locations where the ground surface was flat or regularly sloping, without undulations) was ruled out. Landslides and gravitational movements occurring where the coseismic rupture crossed steep, instable slopes (fig. 4.2.1) were also carefully mapped to avoid the inclusion of surface ruptures due to shallow gravitational collapse in the coseismic slip measurements.

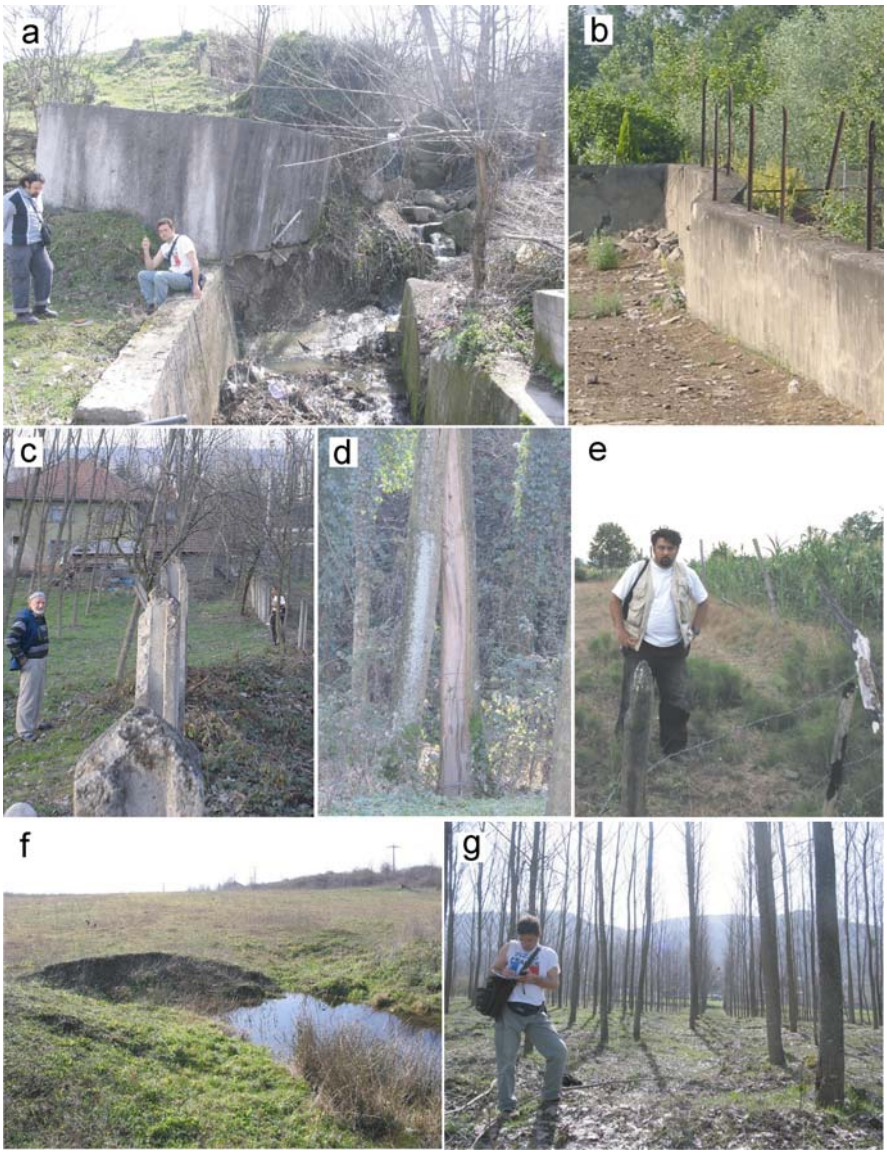

Figure 4.2.5. Examples of piercing point used for coseismic offset extimations: a) offset calcrete levee of a stream;. b) deformed wall; c) offset calcrete fence; d) split tree; e) offset wooden fence; f) offset ridge hingeline; g) offset trees line.

On the basis of sharp changes in the strike direction of the coseismic ruptures, the fault trace in the study area can be divided into four, 3 to 4 km long, subsections. These are named from west to east: the Lake Efteni, Yenikoy, Cinarli, and Beykoy subsections that trend WNW-ESE, WSW-ENE, E-W and WSW-ENE, respectively (fig. 4.2.6a). The ruptures along the first two subsections produced relative subsidence of the block to the north. Conversely, the Cinarli and Beykoy subsections produced topographic offset with relative subsidence of the block to their south (fig. 4.2.6). This had impact on local north-flowing drainages, which were dammed at several points by coseismic scarps across them.

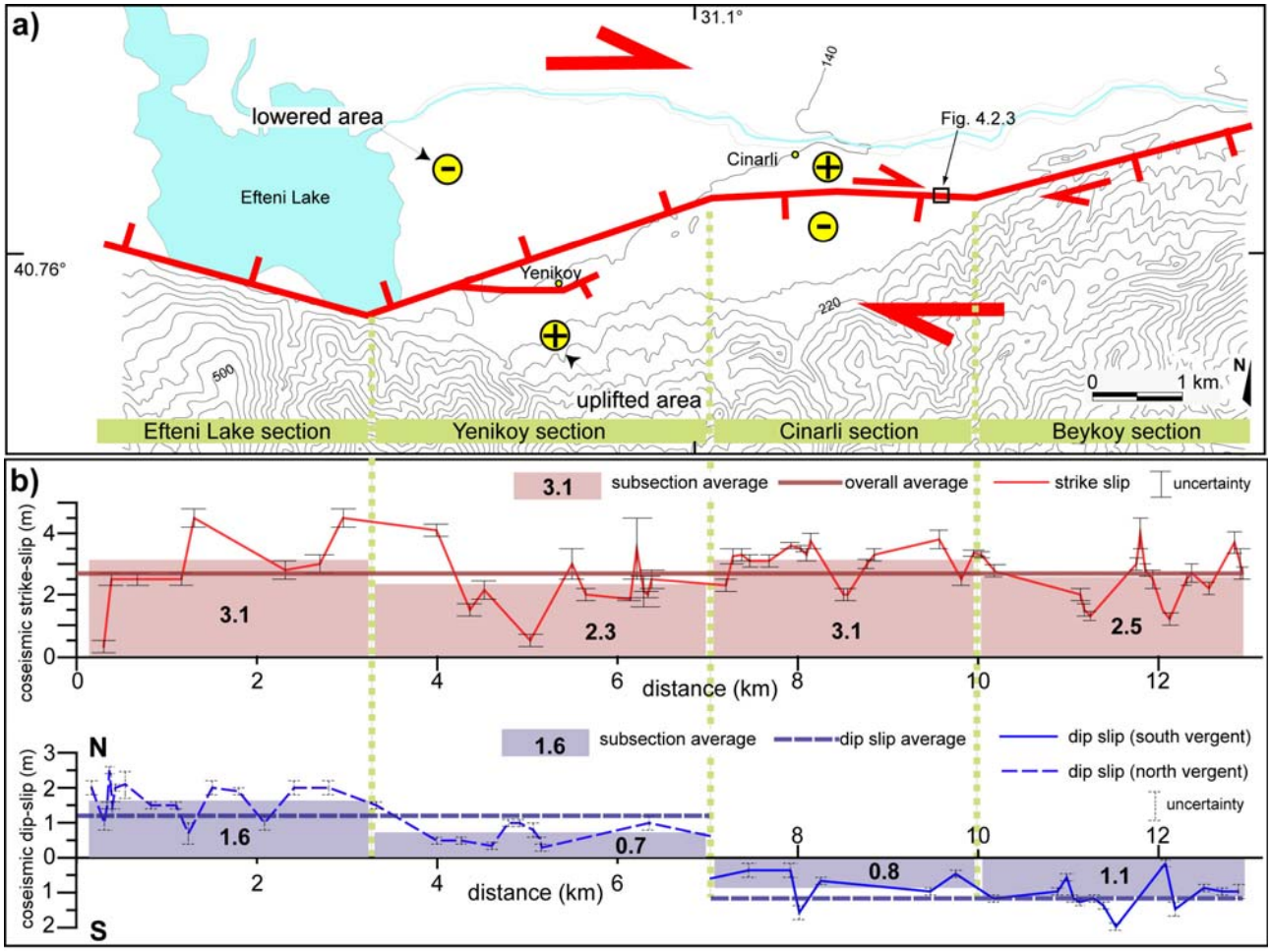

Figure 4.2.6. a) Simplified coseismic fault trace, subdivided into the four subsections on the basis of their strike with respect to the mean strike of the Düzce fault. Contour interval 40 m. b) Horizontal and vertical slip distribution along the coseismic fault trace in the study area. Uncertainties have been evaluated by measuring minimum and maximum of the displacement and their range depends on the type of piercing point used.

Overall, the slip measurements (fig. 4.2.6b, Appendix I-I.i and ii) exhibit a great variability along strike, with 4.5 m maximum dextral offsets (2.7 m average) and 2.5 m maximum vertical offset. The main characteristics of the slip distribution are: (1) the maximum dextral offset of the Efteni Lake is higher than that of the other sections, (2) the average dextral offset of the Efteni Lake and Cinarli subsections is higher than that of the other sections, (3) the vertical component reaches its maximum along the Efteni subsection, (4) the dip-slip direction changes at the boundary between Yenikoy and Cinarli subsections (fig. 4.2.6b). Modeled slip distribution at depth, obtained by joint inversion of GPS and InSAR data, indicates a maximum right-lateral slip of more than 4 m, in the Düzce area [Cakir et al., 2003a; Burgmann et al., 2002]. The great

variability of the strike-slip distribution with points displaying low values could denote losses of slip because of the anastomosing of the rupture, possibly due to scarce connection between the ruptured fault at depth and the surface ruptures (mechanical problems), or because of the plastic deformation in the unconsolidated deposits that overlies the bedrock. If we consider that the coseismic strike-slip distribution at the surface is representative of the movement along the seismogenic fault (see focal mechanism), the maximum dextral offsets, measured at the surface, would better represent the fault slip at depth. This is not true for the coseismic dip-slip at the surface, which includes local components (transtensional or transpressional) and may also contain an unknown component related to gravitational effects (*i.e.*, sediment compaction).

4.2.2. The short- and long-term expression

As already mentioned, one of the reasons for selecting this area for a detailed study was the fact that the 1999 ruptures affected Holocene and Pleistocene deposits. Because of this, the Quaternary deformational history of the Düzce fault can be reconstructed by investigating the setting of their depositional and tectonic landforms. In fact, the generally loose and soft recent deposits can develop well-expressed tectonic morphologies that record persistent landform modification due to faulting. Following this perspective and with the aim of highlighting the short- (Holocene) and long-term (Pliocene-Pleistocene) tectonic setting and evolution of this part of the Düzce fault, geomorphic analysis is conducted, first along the 1999 rupture zone (hereinafter referred as near-fault), then in a broader area around it (hereinafter referred as far-field).

The contribution of gravitational movements to the landform evolution and to the observed relief has been considered with particular attention. Frequently, landslides are responsible for the degradation of the tectonic landforms (*e.g.*, interrupting the continuity of fault escarpments). Most of the landslides, both old and generated by the 1999 earthquake, are located along the fault-related topographical anomalies testifying that in the study area the slope evolution is strongly linked to tectonics.

4.2.2.1. Tectonic landforms in the near-fault

In the following section, the geomorphological expression of the four subsections inferred from the coseismic ruptures (see previous section) is discussed. In fact, this subdivision appears, to fit also the long-term fault trace, since each subsection is associated with homogeneous tectonic landform assemblages that are clearly distinct from those of the adjacent subsections.

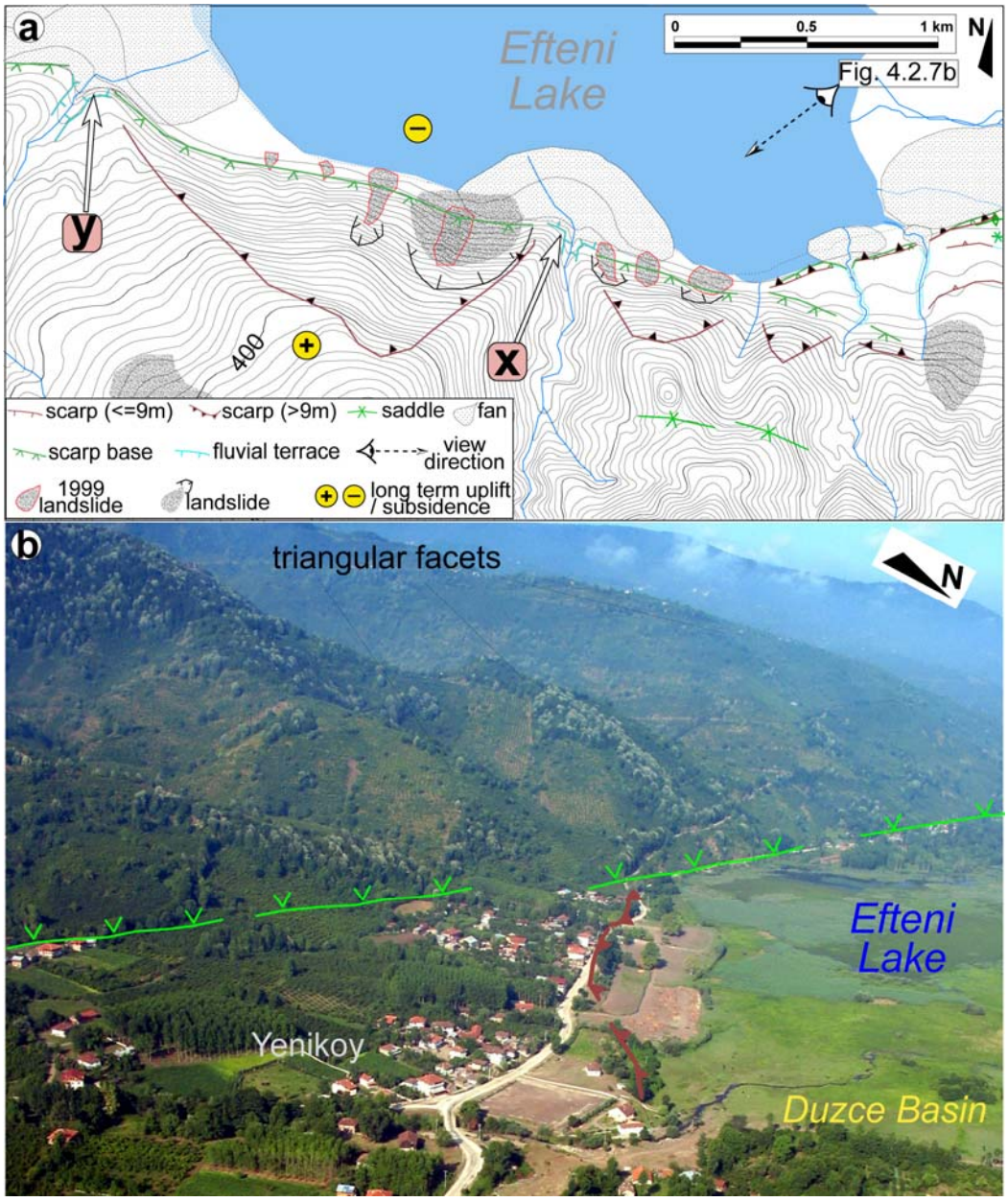

Figure 4.2.7. Cumulative tectonic landforms along the 1999 rupture subsections (see fig. 4.2.1 for location). a) Main tectonic and geomorphological features of the Efteni Lake subsection (see text for explanation). Contour interval 10 m. b) Picture of the triangular facets of the Efteni Lake subsection (see fig. 4.2.7a for view location).

The Efteni Lake subsection of the 1999 ruptures (fig. 4.2.1) coincides with the base of a steep stretch of the Almacik rangefront and is characterised by the lack of well-developed piedmont deposits. NNE-facing triangular facets (fig. 4.2.7) are present along the range, deeply incised by canyons that exhibit hanging terraces at their outlet (x and y in fig. 4.2.7a). This setting is clearly indicative of a narrow fault zone (PDZ) located at the base of the range front, which is characterized by a persistent tectonic activity that subsided the northern block.

The trace of the Yenikoy subsection (fig. 4.2.1) coincides with the northward limit of a composite Pleistocene bajada (*i.e.*, alluvial fans merging into a single apron of sediments that covers the foot of the range), and follows the alignment of the active Holocene fans, deposited in subsequent incisions of the Pleistocene fan surface (fig. 4.2.1). This bajada has a topographic profile with a steep fanhead characterized by an abrupt transition to the fluvio-lacustrine deposits, indicating that the bajada is no longer related to the present dynamics of the Düzce plain. The generally linear contact between the bajada and the plain, is a degraded and indented escarpment, WSW-ENE trending. The presence of this escarpment suggests relative subsidence north of the Düzce fault, a fact further indicated by the stream incisions across the bajada itself. The morphology of the bajada-bounding escarpment, even though dissected by north-flowing drainages, can be subdivided into two main right-stepping elements. The westernmost is a fairly continuous, about 10 m-high, north facing escarpment (from y to z in fig. 4.2.8) that is up to 20 m high in its central part. The eastern element is a substantially higher scarp averaging 15 m, that is more degraded towards the western edge, where is perceptible only as a linear slope gradient variation, but becomes very prominent to the east (from k to w in fig. 4.2.8) where it rises up to 50 m above the Düzce plain (x in fig. 4.2.8). The right step-over, recognised in the escarpment, is also illustrated vividly by morphologic ridges, along the two distinct elements.

These ridges, 300 to 1000 m-long and 10 to 40 m high, have elongated shapes with long axes paralleling the escarpments they are associated with. The ridges have asymmetric cross profiles, with steep northern flanks and gentler south flanks, that express a smooth (ridges 1 and 2 in fig. 4.2.8) or abrupt (ridges 3 and 4 in fig. 4.2.8 and see profile A-A' in inset) transition to the bajada surface. These observations suggest that the Yenikoy subsection is formed by two main, ca. 500 m spaced, WSW-ENE striking, ca. 2 km long right-stepping fault traces (y-z and k-w in fig. 4.2.8) that have been producing uplift of the block to their south.

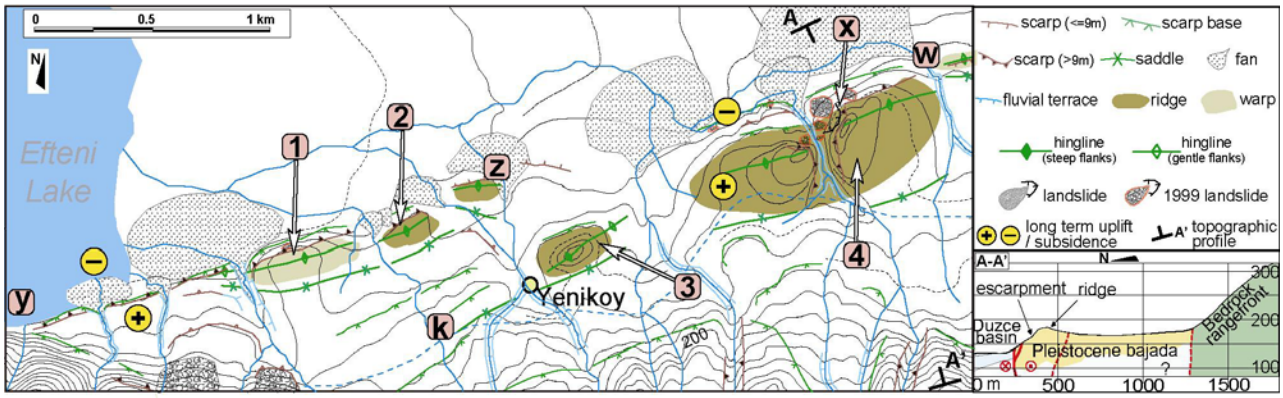

Figure 4.2.8. Cumulative tectonic landforms along the Cinarli subsection (see fig. 4.2.1 for location). Main tectonic and geomorphological features of the Yenikoy subsection (see text for explanation). Contour interval 10 m. The inset shows a simplified cross-section of the escarpment on the Pleistocene bajada deposits that was affected by the 1999 ruptures.

The Cinarli subsection is associated with a prominent, 3 to 15 m high, south-facing escarpment across the bajada deposits (fig. 4.2.1 and fig. 4.2.9a). This ca. E-W trending escarpment is formed by a set of left-stepping en-échelon, 200 to 700 m long and ca. 100 m spaced scarps and constitutes the northern boundary of a flat and depressed area. The escarpment has a topographic profile characterised by a sharp asymmetric warp: a steep and short southern slope contrasts with a gentler northern slope, whose gradient is coincident with the bajada depositional gradient (see profile B-B' in inset of fig. 4.2.9a and fig. 4.2.9b). In some cases, the scarps of the Cinarli subsection act as natural dams for northward flowing drainages, being thus responsible for the formation of ponds, flooding and alluvial deposition. Two of the major dammed areas are drained by large artificial channels (fig. 4.2.9a). In the easternmost part of the subsection, two

escarpment-bounded depressions also trap Holocene pond and fan deposits against the scarp (x in fig. 4.2.9a). North-flowing drainages are characteristically deflected in an apparent left-lateral sense, since they cross the bajada through the escarpment step-overs, where the damming is less effective (*i.e.*, the scarps are less high where they overlap, fig. 4.2.9a). The complex setting described above is suggestive of a set of short, up to 1 km long left-stepping fault strands forming the Cinarli subsection, that have been producing subsidence of the southern block.

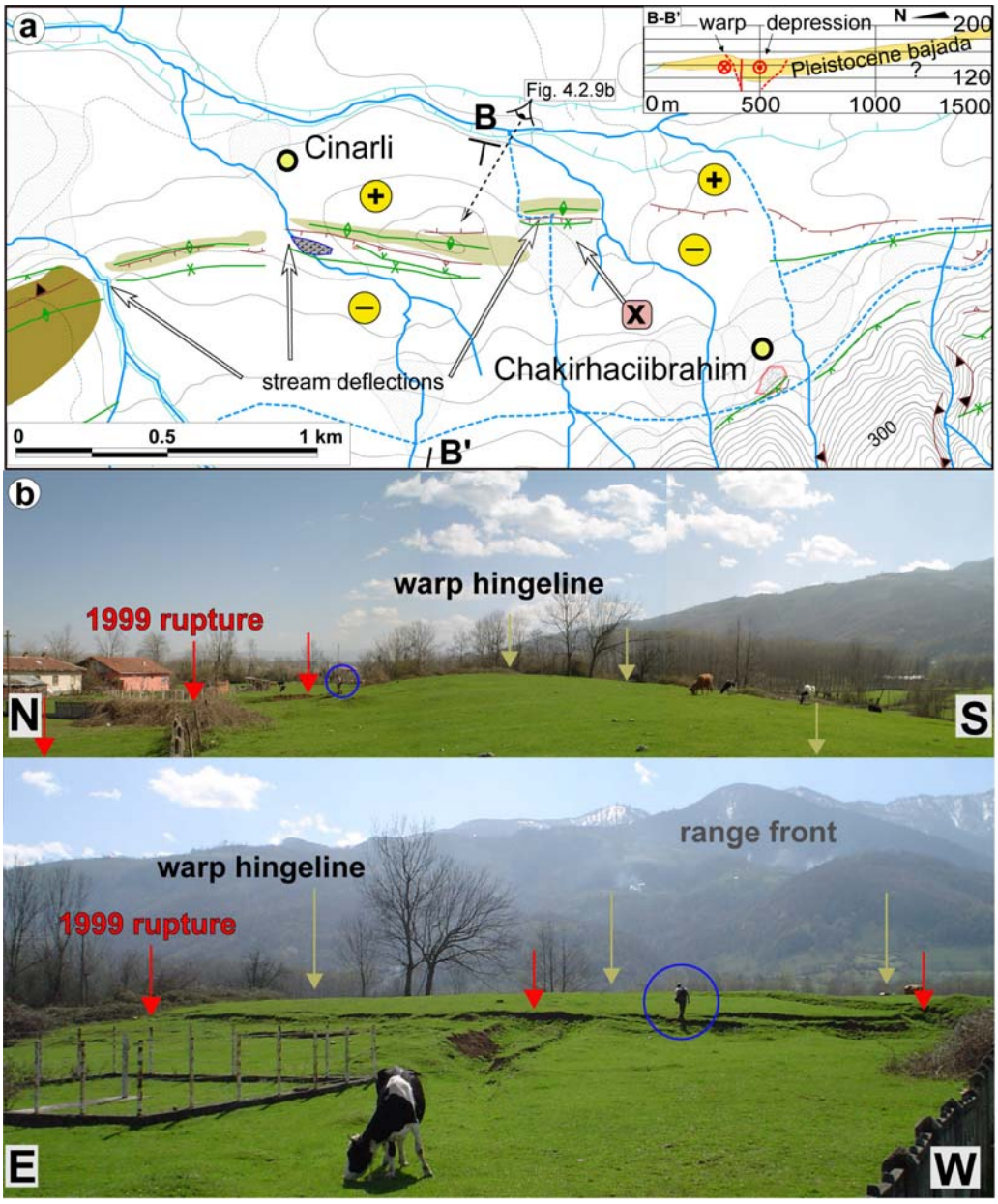

Figure 4.2.9. Cumulative tectonic landforms along the Cinarli subsection (see fig. 4.2.1 for location). a) Main tectonic and geomorphological features of the Cinarli subsection (see text for explanation) (legend same as fig. 4.2.8). Contour interval 10 m. The inset shows a simplified cross-section of the escarpment on the Pleistocene bajada deposits that was affected by the 1999 ruptures. b) Photos of tectonic warp (man in circle for scale) (see fig.4.2.9a for location).

Farther east, the Beykoy subsection contrasts with the Cinarli subsection because it is associated with well-expressed, 400 to 800 m long, WSW-ENE trending elongated tectonic ridges, along the base of the range front (fig. 4.2.1 and fig. 4.2.10). Most of these ridges are made of a Paleozoic-Jurassic granitoid unit, are ca. 70 m high and have symmetric profiles and steep slopes (fig. 4.2.10b). Only one of the eastern ridges is made of recent deposits of a remnant of a Pleistocene bajada. This latter, compared to the bedrock ridges, is lower (30 m high) and asymmetric, with a steep south-facing slope. Narrow and hanging WSW-ENE linear valleys, up to 40 m deep, have developed between the elongated ridges and the base of the range front. The north-flowing drainages show clear anomalies. Right-hand stream deflections of about 130 m (x in fig. 4.2.10a) occurred because of: 1) the growth and offset of the ridges that act as natural dams to their flow; 2) incision of both linear valleys and ridges that forced the streams to maintain their bed; 3) low stream power, that is not strong enough to erode the intervening ridges and to straighten their course. Tectonic influence on drainage patterns is also expressed by stream piracy along the fault (creating apparent sinistral deflections) and perched ponding areas (y and z, respectively in fig. 4.2.10). The setting of the Beykoy section suggests the existence of a WSW-ENE striking, persistent fault trace, located along the linear valley between the ridges and the range-front slope. A secondary parallel fault trace possibly bounds the northern side of the linear ridges, causing its relative uplift with respect to the Düzce plain.

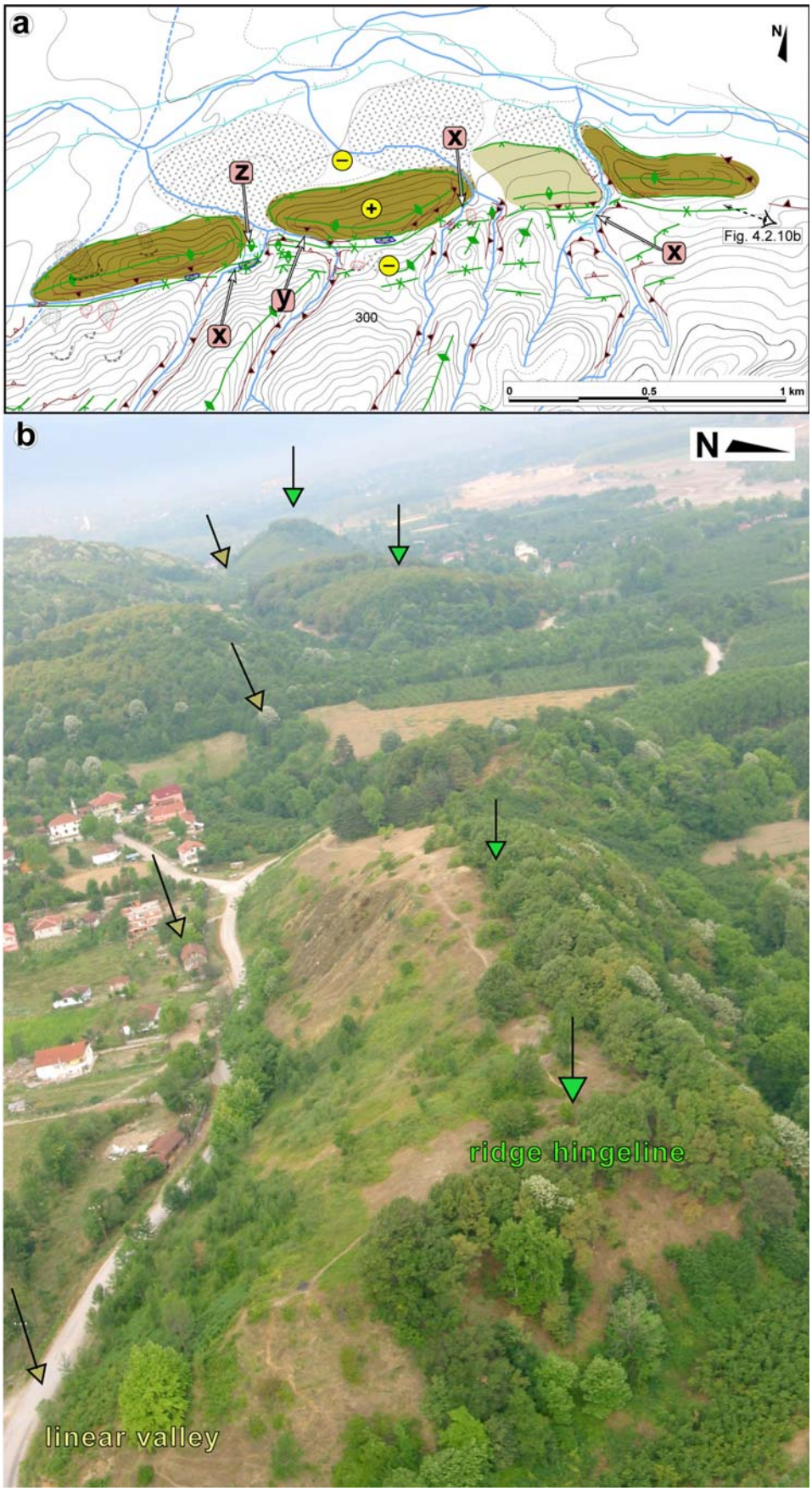

Figure 4.2.10. a) Main tectonic and geomorphological features of the Beykoy subsection (see text for explanation) (legend same as fig. 4.2.8). Contour interval 10 m. b) Aerial view of tectonic ridges (see fig. 4.2.10a for view location).

4.2.2.2. Tectonic landforms in the far-field

To better understand the interaction of faulting and landform and to decipher the fault evolution, we enlarged the area of observation from the near-fault features to a 5-km-wide zone (fig. 4.2.11). In this broader view the short/long-term geomorphic characteristics of the Düzce fault, east of Lake Efteni subsection, indicate that the zone of deformation that separates the Almacik block from the Düzce plain is composed, besides the PDZ, by a complex WNW-ESE and WSW-ENE range front fault system (hereinafter referred to as RFS) (fig. 4.2.12). The Pleistocene bajada is certainly the most significant geomorphic feature highlighting the RFS (fig. 4.2.1). It developed within a ca. 2.5 km wide and 7 km long (b-c-d-f in fig. 4.2.11) fault-controlled triangular embayment of the Almacik range front. In figure 4.2.11, stretch b-f-g of the RFS is essentially the extension towards the ESE of the Lake Efteni fault subsection. In fact, the alignments of linear ridges, valleys (y in fig. 4.2.11) and bases of indented and fairly well preserved facets, up to 250 m high, (x in fig. 4.2.11) eloquently depict a fault. This fault is exposed in one outcrop (z in fig. 4.2.11), where facet-parallel, right-lateral fault planes juxtapose Late Eocene against Paleozoic-Jurassic units (see fig. 4.2.1).

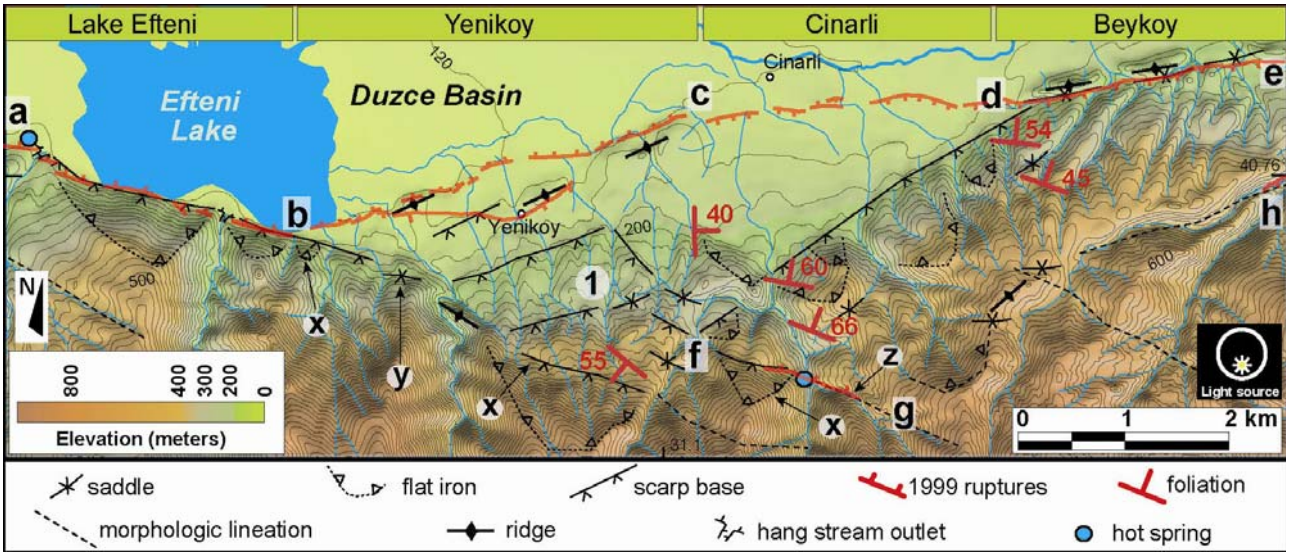

Figure 4.2.11. a) Broader scale tectonic geomorphology of the study area. Shaded relief based on digital elevation model (DEM, interpolated from 10 m contours and auxiliary 5 m contours of 1:25.000 scale topographic maps) (see text for explanation). Contour interval 20 m.

The geomorphologic expression of stretch f-d of the RFS is equally clear-cut, as a WSW-ENE straight boundary, characterised by facet-parallel alignments and an abrupt slope gradient change, between the 500 m high range front slopes and the lower relief in front of them (fig. 4.2.12). This WSW-ENE escarpment cannot be attributed to litho-structural control, since foliation and lineation of the outcropping bedrock strike oblique to range front (fig. 4.2.11). In addition, WSW-ENE trending fault planes in bedrock outcrops along the escarpment were observed. Even though clear kinematic indicators could not be identified in these fault outcrops, on the basis of their orientation with respect to the Düzce fault stress field, a transpressive character for the stretch f-d of the RFS can be inferred (fig. 4.2.12). Smaller morphological discontinuities are suggestive of the presence of several minor faults inside this major embayment, bounding a sector of bedrock of intermediate elevations (1 in fig. 4.2.11 and X in fig. 4.2.12).

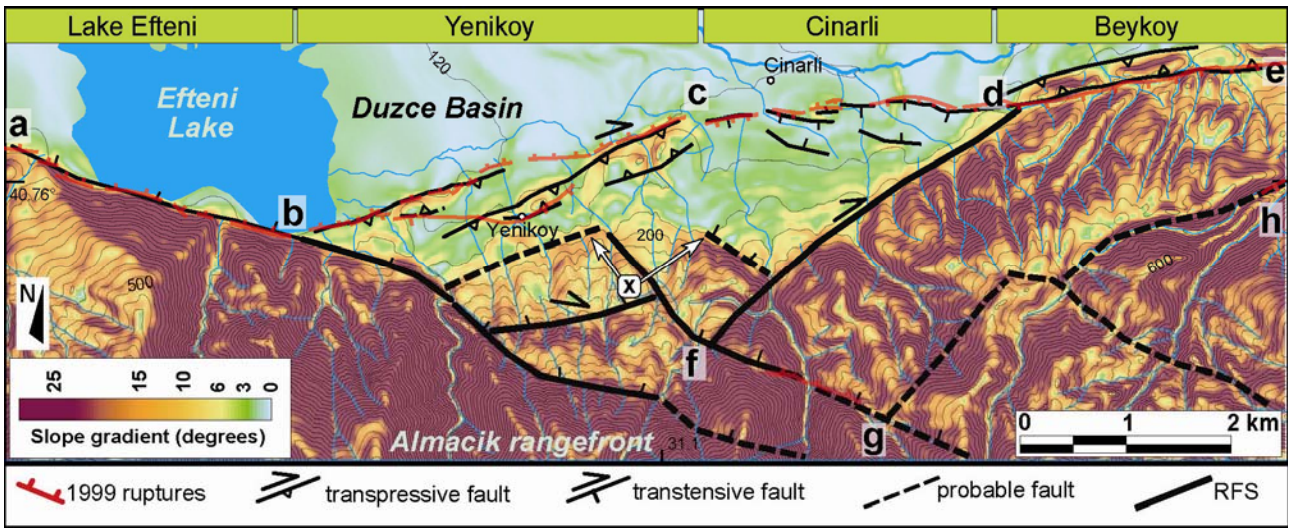

Figure 4.2.12. Slope gradient map from DEM and long-term fault system of the study area. Contour interval 20 m.

Evidence for faulting along the WSW-ENE trending strands of the RFS (g-h in fig. 4.2.12) was also found within the bedrock units. In general, the geomorphic expression of the g-h strand and the lack of fault-controlled recent deposition do not constrain its present activity, but Akyuz et al. [2002] reported up to 15 cm right-lateral offset ruptures along its easternmost part (fig. 4.2.12).